# Ketamine potentiates a glutamatergic presynapse

Abdelmoneim Eshra[1,#], Noa Lipstein[2] and Stefan Hallermann[1,#]

[1] Carl-Ludwig-Institute for Physiology, Medical Faculty, University of Leipzig, Liebigstrasse 27, 04103 Leipzig, Germany
[2] Leibniz-Forschungsinstitut für Molekulare Pharmakologie (FMP), 13125 Berlin, Germany
[#] correspondence: Abdelmoneim.Eshra@medizin.uni-leipzig.de and hallermann@medizin.uni-leipzig.de

## Abstract

Ketamine is a NMDA receptor blocker with rapid antidepressant effects that are mediated by increased glutamatergic signalling. It remains unclear whether ketamine increases presynaptic function itself or acts via postsynaptic or network-level-mechanisms. Using presynaptic capacitance measurements at acute brain slices, we show that ketamine enhances presynaptic function within minutes. The presynaptic potentiation persisted >30 minutes after washout of ketamine and did not occur with MK-801, another NMDA receptor blocker. Mechanistically, ketamine increased both calcium influx and the number of release-ready vesicles. Our data uncover a rapid effect of ketamine on key presynaptic properties of glutamatergic signalling.

The rapid and sustained antidepressant effect of ketamine after a single dose may represent the biggest breakthrough in the field of psychiatry in the last 50 years[1,2]. There is general agreement that ketamine is an open channel blocker of N-methyl-D-aspartate receptors (NMDARs), that induces a glutamate surge and persistent potentiation of glutamatergic signalling via neural plasticty[3–7]. However, the origin of the potentiation of glutamatergic synapses after ketamine application remains unclear[3].

Ketamine-induced functional and structural plasticity has been extensively described in the postsynaptic context. For example, a prominent theory for the potentiation of glutamatergic signalling is that ketamine disinhibits glutamatergic neurons by preferentially blocking NMDARs on GABAergic neurons[3,4,6]. This is sometimes called the "presynaptic effect" but refers to increased neuronal activity of glutamatergic neurons rather than to direct effects of ketamine on presynaptic nerve terminals. Another prominent theory is that ketamine induces postsynaptic amplification of glutamatergic synapses by preferentially blocking NMDARs that mediate spontaneous neurotransmission[8]. However, in general the presynaptic contribution to the enhancement of glutamatergic signalling remains elusive and controversial[9–11]. This is partially due to technical limitations. To our knowledge, all previous electrophysiological studies of ketamine relied on postsynaptic measurements. In addition to the general limitations of relying on postsynaptic recordings to interpret presynaptic function, the case of ketamine is further complicated by its NMDAR-blockade, which may alter postsynaptic readouts. Moreover, the increased neuronal activity of glutamatergic neurons makes it difficult to disentangle direct effects of ketamine on glutamate release, intrinsic to the presynaptic terminal, from indirect effects on glutamate release due to increased network activity.

To isolate the presynaptic effects of ketamine, we conducted high-resolution presynaptic patch-clamp recordings and capacitance measurements[12] at the cerebellar mossy fibre synapse. Such measurements allow to directly monitor presynaptic release independent of postsynaptic receptors and of axonal mechanisms that may influence presynaptic action potentials. In addition, the cell soma can be removed by cutting the axon during slice preparation (Fig. 1a), allowing us to isolate the immediate effects of ketamine on presynaptic terminals, independent of upstream

effects occuring at the cell soma which may lead to increased neuronal network activity.

We applied depolarizing pulses of increasing duration from 1 to 100 ms in ketamine or control conditions. In the presence of ketamine (50 µM) for an average of 30 min, we observed larger depolarization-evoked capacitance increase indicating enhanced glutamate release (Fig. 1a). To probe the sustained effects after ketamine removal, we incubated brain slices with ketamine (50 µM) for 30 min, then transferred the slices to a drug-free solution where the recordings were performed after approximately 30 min of washout. A similar enhancement of release was observed after the washout of ketamine indicating that the enhancement of presynaptic release persists for at least 30 min (Fig. 1b). The mean value of the 10-ms-evoked capacitance jumps normalised to resting capacitance ($\Delta C_m/C_m$) was >50% greater in ketamine-treated nerve terminals compared to control conditions (Fig. 1b).

To analyze if NMDARs-blockade in general potentiates presynaptic release, we applied MK-801 which is another open-channel blocker of NMDARs, having the same channel binding domain but with longer trapping time. Interestingly, slice incubation for 30 min in 50 µM MK-801 had no effect on presynaptic release (Fig.1c). We confirmed the blocking effect of MK-801 on pharmacologically isolated NMDAR-currents (data not shown). The clinically-relevant ketamine concentrations in the brain are thought to be closer to 10 than 50 µM[13]. We therefore conducted a set of experiments using 10 µM ketamine or 10 µM MK-801 applied for 30 min, followed by approximately 30 min of washout (Fig. 1d). Again only ketamine but not MK-801 enhanced presynaptic glutamate release indicating that clinically-relevant ketamine concentrations cause presynaptic potentiation that is not caused by simple blockade of NMDAR.

Analysing the steady-state amplitude of the pharmacologically isolated presynaptic calcium currents eliciting the capacitance jumps (Fig. 2a) showed that in all datasets, in which ketamine was used, the calcium current density showed trend towards higher amplitudes (Fig. 2b). When data from all experimental groups were pooled, regardless of concentration or method of drug administration, a significant increase in calcium current density was observed in ketamine-treated boutons (Fig. 2b). Given the calcium-release power relationship at this synapse[12], a slight increase in calcium influx could

explain the enhanced release we observed with ketamine. We therefore analyzed the relationship between release and calcium influx by plotting $\Delta C_m/C_m$ versus calcium charge density and fitted these relationships with biexponential functions to describe the coupling between calcium and release (Fig. 2c-f). If the enhancement of presynaptic release was simply due to more calcium influx, the ketamine data points should lay on the biexponential fit curve of the control data (i.e. shifted towards more calcium influx and more release within the normal calcium-release relationship). In contrast, we found that ketamine, but not MK-801, resulted in a profound upward shift of the overall relationship (Fig. 2c-f), indicating that the efficiency of glutamate release upon calcium influx is increased by ketamine application. Therefore, our data indicate that ketamine increases both presynaptic calcium influx and the efficiency of calcium-release coupling.

In summary, we demonstrate a rapid and surprisingly profound increase in presynaptic release based on 238 technically challenging direct presynaptic patch-clamp recordings in acute slices from four independent sets of experiments. Although the time scale of 30 min to one hour in our study is much shorter than the time scale of days for antidepressant effects of ketamine in patients, the here-observed enhanced presynaptic release demonstrates that ketamine induces a long-lasting presynaptic plasticity[14]. The increased glutamate release might contribute to the glutamate surge observed in patients, which is thought to induce neuronal-circuit potentiation that mediates the antidepressant effects of ketamine[4–6]. However, further studies are needed to investigate the direct link between presynaptic potentiation and antidepressant effects of ketamine.

Our data indicate that ketamine increases the number of release-ready vesicles rather than the release probability, because an increase in release probability should only potentiate release at depolarizations with short duration. Instead, ketamine potentiated release at all depolarization durations (1-100 ms). Our results are therefore consistent with studies showing no efffect of ketamine on paired-pulse ratio of postsynaptic currents[11]. This often-used assessment of presynaptic strength is insensitive to changes in the number of release-ready vesicles. An increase in the number of release-ready vesicles is furthermore consistent with alterations of presynaptic

vesicular proteins upon ketamine application[4,15,16], but this could also be due to indirect effects of elevated neuronal network activity.

Our finding that only ketamine but not MK-801 potentiates presynaptic function argues for an NMDAR-independent mechanism. Consistently, ketamine and MK-801 can differentially modulate cAMP and BDNF signalling[17]. However, a role of NMDARs in the here-observed presynaptic potentiation cannot be fully excluded. Ketamine and MK-801 have different trapping time at the NMDAR, which might induce different current time courses or metabotropic-like effects[18]. At the cerebellar mossy fiber synapse, a similar increase in glutamate release was recently observed upon homeostatic plasticity via blockade of postsynaptic AMPA receptors[19]. Our MK-801 data argue against simple homeostatic plasticity as the cause of ketamine's presynaptic potentiation, but more complicated forms of presynaptic homeostatic plasticity that depend on the used drug to block postsynaptic receptors[20] could mediate the presynaptic potentiation.

Interestingly, at CA3 neurons, ketamine has been shown to enhance the release probability in a HCN1 channel-dependent manner[9]. Our results cannot be explained by a modulatory effect of ketamine on HCN1 function because the here-used voltage-clamp mode excludes effects of HCN channels on excitability[21]. Furthermore, the metabolic product of ketamine, hydroxynorketamine (HNK), has been shown to mediate presynaptic strengthening[22]. However, our results can also not be explained by the action of HNK because we applied ketamine directly to the brain tissue therefore excluding the metabolic pathway through the liver. Therefore, the here-described direct presynaptic potentiation is independent of postsynaptic signal amplification via NMDAR-blockade, circuit potentiation, NMDAR-dependent disinhibition, or ketamine metabolism, but could operate synergistically with these indirect mechanisms[3,4,8].

In conclusion, our data show that ketamine rapidly potentiates presynaptic function, therefore providing a novel mechanism for the ketamine-induced glutamate surge in patients. These results open up new avenues of research to address the urgent need for side effect-free rapid-acting antidepressants.

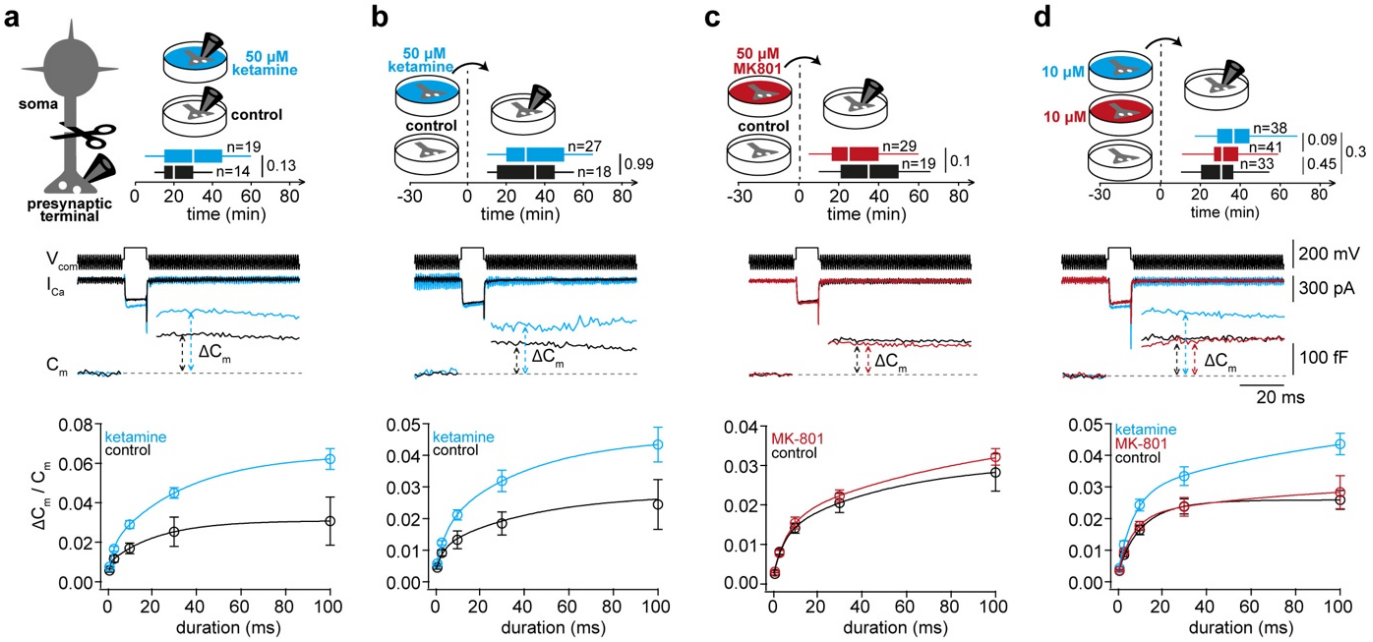


**Fig. 1 Ketamine but not MK-801 enhances glutamate release**

(a) *Top left:* Pictogram of the recording configuration of the presynaptic terminal with a cut axon. *Top right:* Illustration of the continuous application of 50 µM ketamine (blue) or control solution (black). The corresponding time of application is provided as horizontal box plots. *Middle:* Example traces of the voltage command used for the capacitance recordings, the pharmacologically isolated calcium current, and the depolarization-evoked capacitance increase. *Bottom:* Average $\Delta C_m$ normalized to resting capacitance versus depolarization duration.
(b) Same as in panel a but for an experimental set where ketamine (50 µM, blue) or control solution (black) was applied for 30 min before washout. The corresponding time of washout before the bouton recordings in the drug-free solution is provided as box plots.
(c) Same as in panel b but for MK-801 (50 µM, red) and control solution (black).
(d) Same as in panel b but for ketamine (10 µM, blue), MK-801 (10 µM, red), and control solution (black).

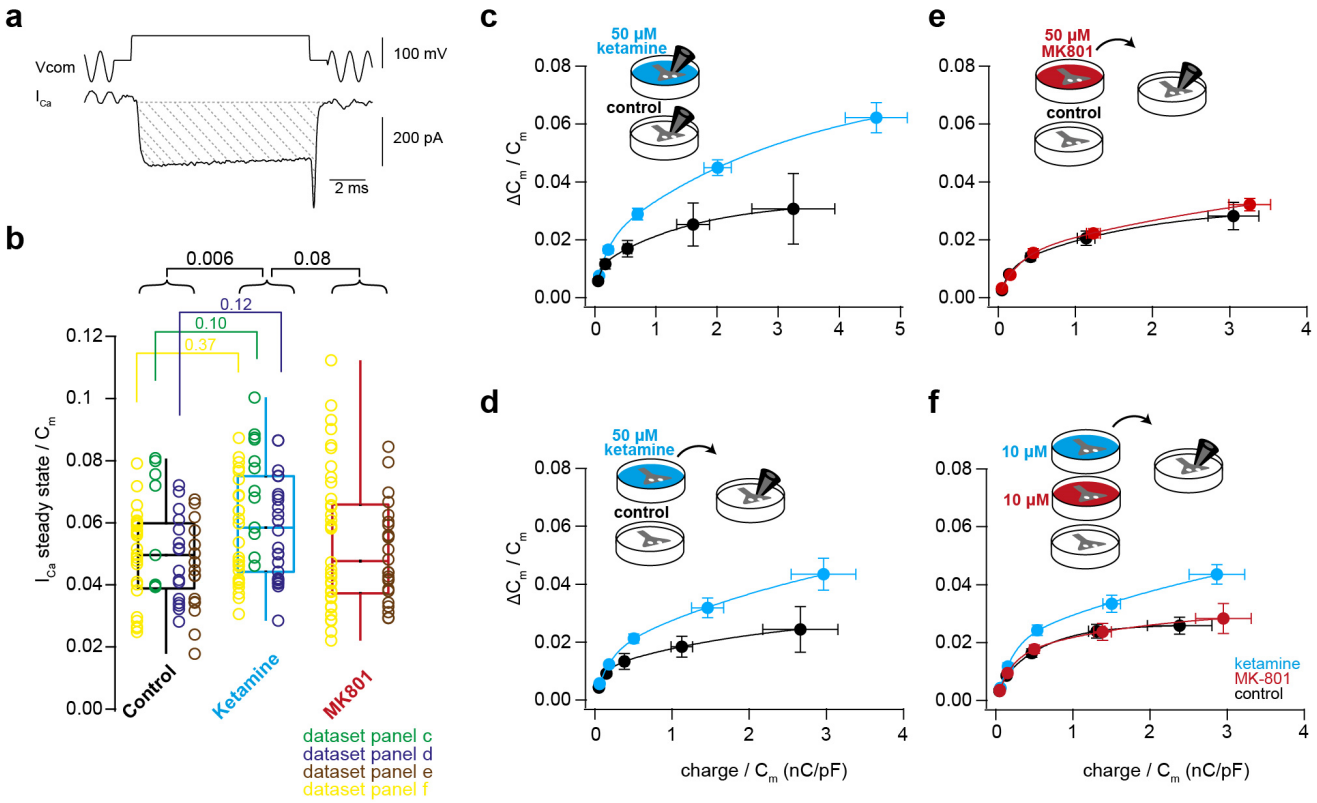


**Fig. 2 Ketamine enhances presynaptic calcium influx and calcium-release coupling**

(a) *Top:* Voltage command, *Bottom:* Calcium current. Dashed lines indicate the integral of the calcium current to measure the charge transfer.
(b) Steady-state calcium current density evoked by 3-ms-pulses from all experimental groups shown in Fig. 1. Color code represents different independent experimental groups. Boxplots show median and interquartile range with whiskers indicating minimum/maximum. Values of individual experiments are superimposed as circles. The numbers above the boxplots represent P-values as explained in the methods.
(c-f) Plot of average $\Delta C_m$ normalized to resting capacitance versus average charge density for experimental sets illustrated in (Fig. 1a-d).

## Supporting Information

## Supporting dataset

| Fig. | Drug | Number of recordings | | | | | | P-value two-way ANOVA | P-value Tukey post hoc test vs. control |
|---|---|---|---|---|---|---|---|---|---|
| | | all | 1ms | 3ms | 10ms | 30ms | 100ms | | |
| 1a | Control | 14 | 13 | 9 | 8 | 6 | 4 | <0.001 | |
| | Ketamine | 19 | 18 | 12 | 10 | 8 | 8 | | <0.001 |
| 1b | Control | 18 | 16 | 15 | 8 | 7 | 6 | <0.001 | |
| | Ketamine | 27 | 21 | 24 | 17 | 11 | 11 | | <0.001 |
| 1c | Control | 19 | 17 | 16 | 13 | 11 | 11 | 0.15 | |
| | MK-801 | 29 | 28 | 24 | 19 | 17 | 17 | | 0.15 |
| 1d | Control | 33 | 31 | 28 | 19 | 13 | 10 | <0.001 | |
| | Ketamine | 38 | 31 | 27 | 20 | 16 | 16 | | <0.001 |
| | MK-801 | 41 | 37 | 34 | 25 | 18 | 13 | | 0.73 |
| 2c | Control | 14 | 13 | 9 | 8 | 6 | 4 | | |
| | Ketamine | 19 | 18 | 12 | 10 | 8 | 8 | | |
| 2d | Control | 18 | 16 | 15 | 8 | 7 | 6 | | |
| | Ketamine | 27 | 21 | 24 | 17 | 11 | 11 | | |
| 2e | Control | 19 | 17 | 16 | 13 | 11 | 11 | | |
| | MK-801 | 29 | 28 | 24 | 19 | 17 | 17 | | |
| 2f | Control | 33 | 31 | 28 | 19 | 13 | 10 | | |
| | Ketamine | 38 | 31 | 27 | 20 | 16 | 16 | | |
| | MK-801 | 41 | 37 | 34 | 25 | 18 | 13 | | |

| Fig. | Drug | Number of recordings | P-value Kruskal-Wallis test | P-value DSCF post hoc test vs. ketamine | P-value one-way ANOVA | P-value Tukey post hoc test vs. ketamine |
|---|---|---|---|---|---|---|
| 2b | Control | 68 | 0.007 | 0.006 | 0.006 | 0.004 |
| | Ketamine | 63 | | | | |
| | MK-801 | 58 | | 0.08 | | 0.14 |

**Number of boutons recorded per dataset and statistics.** Only recordings, where both calcium current and capacitance measurements could be analyzed, were included. In cases where the signal to noise ratio was not sufficient, clamping issues occurred, or the seal became leaky, the recording of the corresponding depolarization pulse was excluded. Therefore, the number of recordings varied among different depolarization pulses applied to each recorded bouton. For details on the statistics see methods.

## Extended methods

### Preparation

Animals were treated in accordance with the German Protection of Animals Act and with the guidelines for the welfare of experimental animals issued by the European

Communities Council Directive. Acute cerebellar slices were prepared from mature P35–P42 C57BL/6 mice of either sex as previously described[12]. Animals were anesthetized by isoflurane using a Dräger Vapor 2000 vaporizer (Dräger, Germany) and then sacrificed by decapitation. The cerebellar vermis was quickly dissected and mounted in a chamber filled with ice-cold artificial cerebrospinal fluid (ACSF). Parasagittal slices having a thickness of 300 µm were cut using a Leica VT1200 microtome (Leica Microsystems), transferred to an incubation chamber at 35 °C for ~ 30 min, and then stored at room temperature until experiment time. The ACSF solution for slice cutting and storage contained (in mM) the following: NaCl 125, $NaHCO_3$ 25, glucose 20, KCl 2.5, 2, $NaH_2PO_4$ 1.25, $MgCl_2$ 1 (310 mOsm, pH 7.3 when equilibrated with Carbogen [95% (vol/vol) $O_2$/5% (vol/vol) $CO_2$]).

**Presynaptic recordings**

Recordings were performed at physiological temperature as described[12]. Borosilicate glass (2.0/1.0 mm outer/inner diameter; Science Products) was used to pull presynaptic patch-pipettes to an open-tip resistance of 3-5 MΩ (when filled with intracellular solution) using a DMZ Puller (Zeitz-Instruments, Germany). During recording, slices were superfused with ACSF containing (in mM): NaCl 105, $NaHCO_3$ 25, glucose 25, TEA 20, 4-AP 5, KCl 2.5, $CaCl_2$ 2, $NaH_2PO4$ 1.25, $MgCl_2$ 1, and tetrodotoxin (TTX) 0.001, equilibrated with 95% $O_2$ and 5% $CO_2$. Cerebellar mossy fiber boutons were visualized with oblique illumination and infrared optics. Whole-cell patch-clamp recordings of cerebellar mossy fiber boutons were performed using a HEKA EPC10/2 amplifier controlled by Patchmaster software (HEKA Elektronik, Germany). All recordings were restricted to lobules IV–V of the cerebellar vermis to reduce potential functional heterogeneity among different lobules. The intracellular solution contained (in mM): CsCl 130, $MgCl_2$ 0.5, TEA-Cl 20, HEPES 20, $Na_2ATP$ 5, NaGTP 0.3, Fluo5F 0.05, ATTO-594 0.01.

Capacitance measurements were performed at a holding potential of −100 mV with sine-wave stimulation (5 kHz and ±50 mV amplitude). During the sine wave stimulation, a brief depolarizing pulse was applied. Using an automated protocol written in Patchmaster, consecutive stimulations were performed and the duration of the depolarizing pulse in each stimulation was increased gradually (1, 1, 3, 10, 30, 100 ms). The duration between consecutive capacitance measurements was 15 s for the

weak pulses (1 and 3 ms) and 30 s between the stronger pulses (10, 30, and 100 ms). To make sure that the waiting time between pulses is sufficient and that consecutive stimulation did not induce some sort of facilitation, we compared two consecutive 1 ms pulses at the beginning of each recording and found no difference. The hydrostatic pressure in the patch pipette was kept at zero mbar.

**Drug application**

For incubation experiments (Fig. 1b-d), brain slices were incubated with the drug of interest (ketamine or MK-801) at room temperature. After 30 min, the brain slice was transferred to a drug-free solution for a first washout step of about 10 s. Then, the slice was transferred to the recording chamber to perform electrophysiology at physiological temperature while being continuously perfused with ketamine-free (and MK-801-free) extracellular solution. For experiments where the drug was continuously applied during recording (Fig. 1a), 50 µM ketamine was all the time included in the extracellular solution used for recording.

**Data analysis**

All recordings and the corresponding data analyses (Figs 1, 2) were performed interleaved and blinded. To this end, for each data set the aliquots of ketamine, MK-801, or ACSF were randomly, sequentially numbered by a second person and subsequentally added by the investigator. Unblinding was done after finishing the analyses. Analyses of capacitance measurements and calcium currents were performed using Patchmaster. To quantify the amplitude of capacitance jumps, we measured the difference between a baseline resting capacitance and the depolarization-evoked capacitance jump. The baseline capacitance was measured as the average capacitance during a time frame of 20-60 ms before the depolarizing pulse. The depolarization-evoked capacitance was quantified as the average capacitance during a time frame of 50-100 ms measured 20-30 ms after the end of the depolarizing pulse. Similarly, calcium current amplitudes were quantified by measuring the difference between a baseline (measured as the average current during a time frame of 2-20 ms before the depolarizing pulse) and a steady state current (measured as the average current during a time frame of 0.3-3 ms measured 0.5-3 ms after the end of the depolarizing pulse). Calcium charge transfer was obtained by integrating the current over the entire depolarizing-pulse duration. Lines in Fig.1 (bottom plots)

and Fig. 2 (c-f) represent biexponential fits and the data are shown as mean with error bars denoting standard error of the mean.

### Statistics

For statistical comparisons of the data in Fig. 1 and Fig. 2c-f, we perform two-way ANOVA and Tukey post hoc tests. For the data in Fig. 2b, a non-parametric one-way ANOVA (Kruskal–Wallis) test with non-parametric post hoc tests (Dwass–Steel–Critchlow–Fligner pairwise comparisons; DSCF) were used, but identical statistical significance levels were obtained with a parametric one-way ANOVA test and Tukey post hoc tests. For comparison of the individual data sets in Fig. 2b, Mann-Whitney U tests were used (color-coded P values are provided in the figure). The calculations were performed with jamovi (www.jamovi.org). See supporting dataset for P-values.

## Author contributions

AE conceptualized the project, designed and performed experiments, and analyzed data. SH supervised the study. AE, NL, and SH wrote the manuscript.

## Acknowledgments

We would like to thank Stephen M. Smith, Volker Haucke, Christian Geis, and Jana Nerlich for critically reading the manuscript and Claudia Binder for technical assistance. This work was supported by the European Research Council (ERC Consolidator Grant 865634) to S.H. and by the German Research Foundation (DFG; FOR 3004 SYNABS, HA6386/10-2 to S.H. and Excellence Strategy EXC-2049-390688087 and CRC 1286 "Quantitative Synaptology" to N.L.).

## Conflict of Interest

The authors declare no conflict of interest.

## References

1. Berman, R. M. *et al.* Antidepressant effects of ketamine in depressed patients. *Biol Psychiatry* **47**, 351–354 (2000).

2. Zarate, C. A. *et al.* A randomized trial of an N-methyl-D-aspartate antagonist in treatment-resistant major depression. *Arch Gen Psychiatry* **63**, 856–864 (2006).

3. Zanos, P. & Gould, T. D. Mechanisms of ketamine action as an antidepressant. *Mol Psychiatry* **23**, 801–811 (2018).

4. Duman, R. S., Aghajanian, G. K., Sanacora, G. & Krystal, J. H. Synaptic plasticity and depression: New insights from stress and rapid-acting antidepressants. *Nat Med* **22**, 238–249 (2016).

5. Moghaddam, B., Adams, B., Verma, A. & Daly, D. Activation of glutamatergic neurotransmission by ketamine: A novel step in the pathway from NMDA receptor blockade to dopaminergic and cognitive disruptions associated with the prefrontal cortex. *Journal of Neuroscience* **17**, 2921–2927 (1997).

6. Krystal, J. H. *et al.* Ketamine and the neurobiology of depression: Toward next-generation rapid-acting antidepressant treatments. *Proc Natl Acad Sci U S A* **120**, (2023).

7. Moda-Sava, R. N. *et al.* Sustained rescue of prefrontal circuit dysfunction by antidepressant-induced spine formation. *Science (1979)* **364**, eaat8078 (2019).

8. Autry, A. E. *et al.* NMDA receptor blockade at rest triggers rapid behavioural antidepressant responses. *Nature* **475**, 91–96 (2011).

9. Zhang, K. *et al.* Essential roles of AMPA receptor GluA1 phosphorylation and presynaptic HCN channels in fast-Acting antidepressant responses of ketamine. *Sci Signal* **9**, ra123 (2016).

10. Lazarevic, V., Yang, Y., Flais, I. & Svenningsson, P. Ketamine decreases neuronally released glutamate via retrograde stimulation of presynaptic adenosine A1 receptors. *Mol Psychiatry* **26**, 7425–7435 (2021).

11. Kim, J. W. & Monteggia, L. M. Increasing doses of ketamine curtail antidepressant responses and suppress associated synaptic signaling pathways. *Behavioural Brain Research* **380**, 112378 (2020).

12. Eshra, A., Schmidt, H., Eilers, J. & Hallermann, S. Calcium dependence of neurotransmitter release at a high fidelity synapse. *Elife* **10**, e70408 (2021).

13. Yang, Y. *et al.* Ketamine blocks bursting in the lateral habenula to rapidly relieve depression. *Nature* **554**, 317–322 (2018).

14. Monday, H. R., Younts, T. J. & Castillo, P. E. Long-Term Plasticity of Neurotransmitter Release: Emerging Mechanisms and Contributions to Brain Function and Disease. *Annu Rev Neurosci* **41**, 299–322 (2018).

15. Crawford, D. C., Ramirez, D. M. O., Trauterman, B., Monteggia, L. M. & Kavalali, E. T. Selective molecular impairment of spontaneous neurotransmission modulates synaptic efficacy. *Nat Commun* **8**, 14436 (2017).

16. Holmes, S. E. *et al.* Imaging the effect of ketamine on synaptic density (SV2A) in the living brain. *Mol Psychiatry* **27**, 2273–2281 (2022).

17. Wray, N. H., Schappi, J. M., Singh, H., Senese, N. B. & Rasenick, M. M. NMDAR-independent, cAMP-dependent antidepressant actions of ketamine. *Mol Psychiatry* **24**, 1833–1843 (2019).

18. Nabavi, S. *et al.* Metabotropic NMDA receptor function is required for NMDA receptor-dependent long-term depression. *Proc Natl Acad Sci U S A* **110**, 4027–4032 (2013).

19. Delvendahl, I., Kita, K. & Müller, M. Rapid and sustained homeostatic control of presynaptic exocytosis at a central synapse. *Proc Natl Acad Sci U S A* **116**, 23783–23789 (2019).

20. Nair, A. G., Muttathukunnel, P. & Müller, M. Distinct molecular pathways govern presynaptic homeostatic plasticity. *Cell Rep* **37**, (2021).

21. Byczkowicz, N. *et al.* HCN channel-mediated neuromodulation can control action potential velocity and fidelity in central axons. *Elife* **8**, e42766 (2019).

22. Riggs, L. M. *et al.* (2R,6R)-hydroxynorketamine rapidly potentiates hippocampal glutamatergic transmission through a synapse-specific presynaptic mechanism. *Neuropsychopharmacology* **45**, 426–436 (2020).